



## CFD Simulation of a Multi-mesh Pulse Tube Regenerator

B. Mousavi<sup>a</sup>, A. A. Alemrajabi<sup>b</sup>, A. Jafarian<sup>\*c</sup>, M. Arablu<sup>d</sup>, A. Behjatian<sup>e</sup><sup>a</sup>Department of Civil Engineering, University of Colorado Denver, Denver<sup>b</sup>Department of Mechanical Engineering, Isfahan University of Technology, Isfahan<sup>c</sup>Department of Mechanical Engineering, Tarbiat Modares University, Tehran<sup>d</sup>Department of Mechanical Engineering, University of North Carolina Charlotte, Charlotte<sup>e</sup>Department of Mechanical Engineering, Southern Illinois University, Carbondale

## P A P E R I N F O

## Paper history:

Received 07 May 2013

Accepted in revised form 18 September 2014

## Keywords:

Pulse Tube

Cryocooler

Multi Mesh Regenerator

Oscillating Flow

## A B S T R A C T

During the last two decades, inertance tube pulse tube cryocoolers (ITPTC) applications in astronautics instruments gained momentum due to their high reliability. Moreover, significant efforts were made in order to improve ITPTCs operation. Investigations showed that most losses occur in the regenerator part. Due to complexity of physics of these losses, effects of the regenerator efficiency on the cryocooler performance were investigated in this work. To calculate heat transfer between solid matrix and acting fluid in the regenerator, Dual Energy Equation (DEE) model was used. Calculation of entropy flow inside the regenerator showed that almost 85% of the energy losses are due to viscous and inertial losses besides most of the energy losses occurring in its hot end. Therefore, in order to optimize the system, multi-mesh regenerator was studied. Results showed that under fixed CHX wall temperature of 150 (K), COP of the PTC with optimum multi-mesh regenerator is 1.07 times higher than the value of uniform mesh regenerator ITPTC. A precise agreement was observed between simulation results and available experimental data published in the literature.

doi: 10.5829/idosi.ije.2015.28.01a.16

## NOMENCLATURES

|                 |  |                      |                                      |
|-----------------|--|----------------------|--------------------------------------|
| $A$             | Heat transfer area (m <sup>2</sup> )                                     | $\vec{v}$            | Velocity vector (m/s)                |
| $C$             | Inertial resistance factor   | $\dot{W}_{pv}$       | P-V power of compressor (W)          |
| $COP$           | Coefficient of performance   | $X_{amp}$            | Amplitude of piston motion (m)       |
| $D_h$           | Hydraulic diameter (m)   | $X_t$                | Screen transvers pitch               |
| $E$             | Local energy (J/kg)  | $x$                  | $x$ axis                             |
| $f_{osc,m}$     | Oscillating friction factor  | $2-D$                | two dimensional                      |
| $\bar{g}$       | Gravity acceleration (N/kg)  | <b>Greek Symbols</b> |                                      |
| $H$             | Local enthalpy (J/kg)  | $\nabla$             | Gradient operator                    |
| $h_{sf}$        | Convective heat transfer coefficient in Porous media (W/m <sup>2</sup> ) | $\rho$               | Density (kg/m <sup>3</sup> )         |
| $k$             | Thermal conductivity (W/m.K)   | $\tau$               | Stress tensor                        |
| $\dot{m}$       | Mass flow rate (kg/s)  | $\mu$                | Dynamic viscosity (Pa.s)             |
| $n$             | Number of packed screens per length                                      | $\beta$              | Darcy permeability (m <sup>2</sup> ) |
| $Nu$            | Nusselt number   | $V$                  | Piston oscillating frequency (Hz)    |
| $p$             | Static pressure (Pa)   | $\mathcal{E}$        | Porosity                             |
| $Pr$            | Prandtl number   | $\phi$               | Opening area ratio of screen         |
| $Re$            | Reynolds number  | <b>Subscripts</b>    |                                      |
| $Re_m$          | Oscillating flow Reynolds number   | $c$                  | Cold heat exchanger                  |
| $R_{osc}$       | Regenerator performance factor (m/s.K)                                   | $f$                  | Fluid                                |
| $S''_{gen,sys}$ | Entropy generation at regenerator (W)                                    | $s$                  | Solid matrix                         |
| $T$             | Temperature (K)  | $sf$                 | Solid-Fluid interface                |
| $t$             | time (s)   |                      |                                      |

\*Corresponding Author's Email : [jafarian@modares.ac.ir](mailto:jafarian@modares.ac.ir) (A. Jafarian)

## 1. INTRODUCTION

Ability to reach very low temperatures with a desired cooling power and high reliability due to omitting the moving part in cold head makes the pulse tube cryocooler (PTC) very useful so that they are widely used in many engineering applications i.e. astronautics, medical and electronic instruments. However, efficiency of the PTC is low and many efforts have been paid to improve that, since its invention by Gifford and Longworth in 1963 [1].

There are many sources of energy loss in PTCs, i.e. viscous and inertial losses and losses due to conduction in solid matrices, etc. However, after four decades of experiences with PTC, it is known that the most of energy losses occur in regenerator part of the system [2]. For the last 10 to 15 years, the regenerator has been the main subject of researches in the cryocooler community due to their complicated flow phenomena of fluid-solid interactions.

Few theoretical and mathematical models have been developed to understand the mechanism of oscillating flow and heat transfer in porous media. Siegel [3] investigated laminar forced convective oscillating flow inside a tube with a uniform heat flux in the tube wall and showed that flow oscillation causes more axial energy transport in the tube. Khodadadi [4] studied the oscillating flow inside the porous media between two parallel plates. In that study, the inertia term in momentum equation and axial conduction in energy equation are neglected but all the other terms are counted. Results of that study showed that flow oscillation causes a phase lag between pressure and velocity which its value decreases by increasing fluid viscosity.

Another important part of losses in the regenerator is pressure drop which affects the flow mechanism and heat transfer between fluid and solid matrices [2]. To achieve an exact heat transfer coefficient in the regenerator, it is necessary to calculate the pressure drop precisely. There have been many efforts to introduce a good relation for friction coefficient in oscillating flow inside the regenerator [5- 13]. Organ's studies [14] showed that there are many differences between oscillating and steady pressure drops in it. Recently, the oscillating friction factors are used in some codes such as Sage Software [11].

Experimental investigations are costly and time consuming. Furthermore, there are many performance details that cannot be easily measured; hence, numerical simulation approach provides comprehensive details which are very useful to understand the flow physics in the PTC; hence, some of the commercial softwares have been recently used to simulate the PTC [15]. However, few 2-D simulations have used DEE model to simulate the heat transfer between fluid and solid matrix in the regenerator [2, 16].

In this study a 2-D axisymmetric CFD model is used to simulate a single stage multi-mesh regenerator ITPTC. Fluent software is used to do the simulations. In order to model the piston motion, Fluent's dynamic meshing function is used. A User Defined Function (UDF) was developed in C programming language to simulate the piston cylinder effect. Both Local Thermal Equilibrium (LTE) and DEE models were used to simulate the heat transfer in the regenerator. Fluent uses LTE model for heat transfer between fluid and solid matrix in porous medium. Therefore, to apply DEE model to the regenerator a User Defined Source (UDS) was developed to add a source term to the energy equation of gas and to simulate the energy equation of solid matrix.

## 2. MATHEMATICAL MODELING, GOVERNING EQUATIONS & CFD SIMULATION CONDITIONS

According to correlations of Brereton and Mankbadi [17] which show the turbulent and laminar regimes border lines for oscillating internal flows, flow is laminar for all parts of the simulated PTC. Thus laminar flow formulation is used in the simulations. Besides, the thermal resistance of all the walls is neglected since these resistances are negligibly small except the wall thickness of the pulse tube section which is extremely important since the heat is transported by the thickness walls using the theory of the surface heat pumping [18]. Hence, the thickness of pulse tube wall is considered.

The continuum based conservation of mass, momentum and energy equations along with the equation of state of the working fluid are as follows [19]:

$$\frac{\partial \varepsilon \rho}{\partial t} + \nabla \cdot (\varepsilon \rho \vec{V}) = 0 \quad (1)$$

$$\frac{\partial \varepsilon \rho}{\partial t} + \nabla \cdot (\varepsilon \rho \vec{V} \vec{V}) = -\varepsilon \nabla p + \nabla \cdot (\varepsilon \tau) + \rho \vec{g} - \left( \frac{\mu}{\beta} \vec{V} + \frac{1}{2} \rho C |\vec{V}| \vec{V} \right) \quad (2)$$

$$\begin{aligned} \frac{\partial}{\partial t} (\varepsilon \rho_f E_f + (1 - \varepsilon) \rho_s E_s) + \nabla \cdot (\vec{V} (\rho_f E_f + p)) \\ = \nabla \cdot (\varepsilon k_f \nabla T + (\tau \cdot \vec{V})) + S \end{aligned} \quad (3)$$

$$p = \rho RT \quad (4)$$

where,  $S = \nabla \cdot ((1 - \varepsilon) k_s \nabla T)$  and  $S = h_{sf} A_{sf} (T_s - T_f)$  are belong to LTE and DEE models, respectively. For the non porous medium:  $\varepsilon = 1$ ,  $\beta = \infty$  and  $C = 0$ , whereas, for the porous mediums  $0 \leq \varepsilon \leq 1$ ,  $\beta \neq \infty$  and  $C \neq 0$ . The energy equation of solid matrix is as follow:

$$(1 - \varepsilon) \frac{\partial}{\partial t} (\rho_s C_s T_s) = (1 - \varepsilon) \nabla \cdot (k_s \nabla T_s) + h_{sf} A_{sf} (T_f - T_s) \quad (5)$$

The UDS boundary condition in the regenerator is shown in Figure 1. Due to high gradient of temperature in the PTC the viscosity and thermal conductivity of the fluid are set as Sutherland formula and polynomial profile of temperature [20], respectively. There are some important sources of entropy generation in the regenerator i.e. interfacial convection, viscous and inertial, matrix and gas conduction etc. Entropy generation in the regenerator is calculated as follow [2]:

$$S''_{gen,sys} = \varepsilon \frac{k_f}{T_f^2} \left( \frac{\partial T_f}{\partial x} \right)^2 + (1 - \varepsilon) \frac{k_s}{T_s^2} \left( \frac{\partial T_s}{\partial x} \right)^2 + \frac{a_{sf} h_{sf}}{T_s T_f} (T_s - T_f)^2 - \varepsilon \frac{V}{T_f} \frac{\partial p}{\partial x} \geq 0 \tag{6}$$

Nusselt number of the oscillating flow in the regenerator is calculated as follow [21]:

For this study 51852 cells were used for meshing. Hybrid mesh (Structured and Unstructured) was selected for girding the domain. The number of cells which is located near walls in oscillating flows is more than one direction flows due to larger velocity gradient near walls. Therefore, the grid network in this study is finer.

$$Nu = \frac{k_f h_{sf}}{D_h} = (1 + 0.99(Re Pr)^{0.66}) \varepsilon^{1.79} \tag{7}$$

Residual amounts in convergence criteria section is set to  $1 \times 10^{-6}$  for continuity, momentum, energy and UDS equations in this CFD simulation. Discretization method for pressure and density (scalar variables) and momentum, energy and UDS (conservation equations) is second-order upwind in this study.

### 3. PHYSICAL MODEL, RESULTS & DISCUSSIONS

To show the simulated results based on multi-mesh regenerator, geometry and operating parameters have been selected from Harvey experimental model [2]. Schematic of simulated PTC is shown in Figure 2. Table 1 shows the characteristics of the system is studying in the present work. Piston head displacement and velocity are set as follows, respectively:

$$X = X_{amp} \sin(2\pi \nu t) \tag{8}$$

$$\frac{dX}{dt} = 2\pi \nu X_{amp} \cos(2\pi \nu t) \tag{9}$$

#### 3. 1. Lowest Attainable Temperature & Efficiency of the PTC & Mesh Independency

In order to validate the accuracy of the simulations first the PTC is simulated under adiabatic and some other fixed temperature condition of CHX wall with both LTE and

DEE models and the results are compared with available numerical and experimental data as shown in Table 2. As shown in Table 2, results of simulations are in very good agreement with experimental data.

Table 3 illustrates the simulation results for different mesh type. With using fine mesh type (71037 cells), the CHX temperature just has a 0.4% reduction; so, for preventing huge calculation costs, the medium mesh type (51852 cells) was chosen for this study.

#### 3. 2. Regenerator Characteristics

In order to investigate the regenerator behavior, results of DEE model under the adiabatic CHX wall condition are considered. Figure 3 shows the pressure variations during a cycle at inlet and outlet of the regenerator. As shown in Figure 3, amplitude of the pressure decreases along the regenerator from inlet to outlet with a little phase shift.

Figure 4 shows variations of fluid and solid matrix temperature during a cycle at  $X/L=0.19$  of the regenerator. Specific heat capacity of solid matrix is higher than fluid heat capacity. Therefore, as shown in Figure 4, amplitude of fluid temperature variations is higher than that corresponds to the solid matrix.

Besides, there are some deviations in the fluid temperature from the sinusoidal form. This deviation is due to flow returning inside the regenerator. When flow returns inside the regenerator the velocity of the fluid decreases and, consequently, convective heat transfer between fluid and solid matrix decreases.

Figure 5 shows velocity variations during a cycle for different sections of the regenerator. As shown in Figure 5, the amplitude of velocity variations in the inlet section of the regenerator is more than that of the outlet section. The decrease in velocity amplitude is due to density increase in the outlet section of the regenerator.

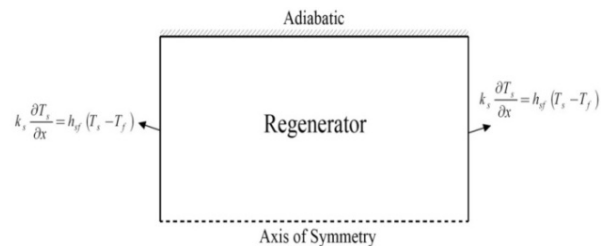


Figure 1. Boundary conditions of UDS in the regenerator

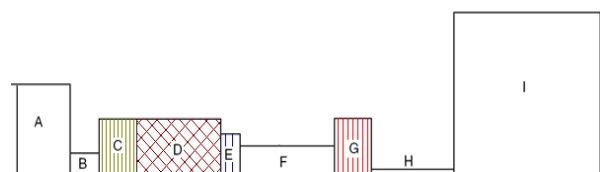


Figure 2. Schematic of the IPTC

**TABLE 1.** Characteristics of the IPTPC, according to Figure 2

| Component               | Radius × length (mm <sup>2</sup> ) | Porous: mesh No. / ε / material | Wall thermal condition         |
|-------------------------|------------------------------------|---------------------------------|--------------------------------|
| Compressor (A)          | 9.54 × 7.5                         | -                               | adiabatic                      |
| Transfer Line (B)       | 1.55 × 101                         | -                               | adiabatic                      |
| After Cooler (C)        | 4 × 20                             | 80 micron / 0.69 / copper       | T=300K                         |
| Regenerator (D)         | 4 × 58                             | 325 / 0.69 / steel              | adiabatic                      |
| Cold Heat Exchanger (E) | 3 × 5.7                            | 80 micron / 0.69 / copper       | adiabatic or fixed temperature |
| Pulse Tube (F)          | 2.5 × 60                           | -                               | adiabatic                      |
| Hot Heat Exchanger (G)  | 4 × 10                             | 80 micron / 0.69 / copper       | T=300K                         |
| Inertance Tube (H)      | 0.43 × 684                         | -                               | adiabatic                      |
| Reservoir (I)           | 13 × 130                           | -                               | adiabatic                      |

**TABLE 2.** Simulation results

| Compon.                | DEE Model (present study) |       |       | LTE Model (present study) |       |        | LTE Model (Ref. 15) |      |      | Exp. (Ref. 2) |
|------------------------|---------------------------|-------|-------|---------------------------|-------|--------|---------------------|------|------|---------------|
| T <sub>c</sub> (K)     | 88*                       | 120   | 150   | 86.5*                     | 100   | 150    | 87*                 | 100  | 150  | 87*           |
| $\dot{W}_{pv}$ (W)     | 62.6                      | 59.8  | 56.8  | 57.2                      | 52.8  | 51.8   | 59.4                | 62.6 | 63.2 | 55            |
| $\dot{Q}_{comp.}$ (W)  | -58                       | -55.6 | -52.4 | -57.4                     | -52.7 | -49.3  | -61                 | -63  | -64  | -             |
| $\dot{Q}_{refig.}$ (W) | 0                         | 6     | 9.4   | 0                         | 2.6   | 11     | 0                   | 1.1  | 6.4  | 0             |
| $\dot{Q}_{rej.}$ (W)   | -7.3                      | -9.1  | -12.2 | -2.5                      | -6.4  | -10.19 | -1.2                | -2.8 | -7.7 | -             |
| COP                    |                           | 0.1   | 0.16  | -                         | 0.05  | 0.21   | -                   | 0.02 | 0.1  | -             |

\* These values are calculated under adiabatic CHX condition.

**TABLE 3.** Characteristics of the IPTPC, according to Figure 2

| Mesh Type   | Number of Cells | CHX Temperature (K) |
|-------------|-----------------|---------------------|
| Coarse Mesh | 16911           | 104                 |
| Coarse Mesh | 37037           | 91                  |
| Medium Mesh | 51852           | 86                  |
| Fine Mesh   | 71037           | 85.63               |

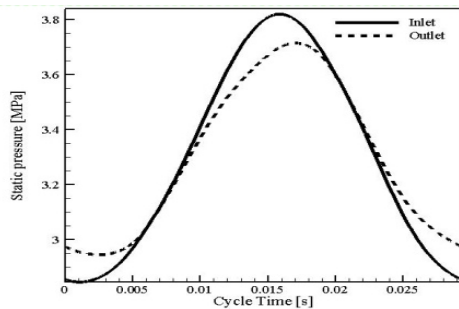


**Figure 3.** Pressure profile at regenerator inlet and outlet during a cycle under adiabatic CHX wall

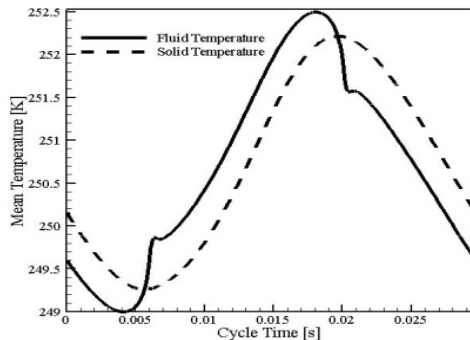


**Figure 4.** Fluid and solid matrix temperature profiles at X/L=0.19 of the regenerator during a cycle

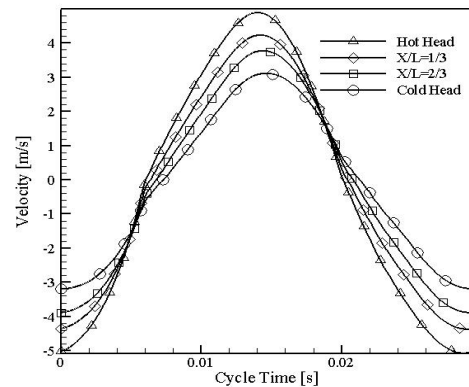


**Figure 5.** Velocity profiles at various sections of the regenerator

If Yuan et al. [22] correlations are used for friction factor and Reynolds number of the oscillating flow ( $Re_m$ ), for the regenerator with uniform mesh#325 under frequency of 34 Hz, the friction factor reads from results of simulations as follow:

$$f_{osc,m} = \frac{102.9}{Re_m} - 0.5439 \quad \text{for } 20 < Re_m \leq 150 \quad (10)$$

Figures 6- A, B, C and D show cyclic average of Reynolds number, Nusselt number, interfacial heat transfer coefficient and friction factor vs.  $Re_m$  along the regenerator, respectively.

As shown in Figures 6- A to C, the values of Reynolds and Nusselt numbers increase along the regenerator from the hot towards the cold end; whereas, the convective heat transfer coefficient decreases along

the same line. The decrease of the density of the fluid and the increase of the viscosity in the cold end are the main reasons that trigger the increase of the Re and Nu. However, a decrease of convective heat transfer coefficient in the cold end is due to a very sharp decrease of helium thermal conductivity.

Figure 7 shows cyclic average of different sources of entropy generation along the regenerator. As shown in Figure 7, the most part of entropy generation (almost 85% of total) belongs to viscous and inertial effect [23, 24]. Furthermore, the entropy generation in the hot end of the regenerator is more than the values corresponding to the cold end. Accordingly, by decreasing the viscous and inertial entropy generation in the hot end of the regenerator, its operation and efficiency improves. This is the main goal of using multi-mesh porous medium in the regenerator parts which is investigated in coming section.

**3. 3. Multi-mesh Regenerator**

As before mentioned most of the regenerator losses occur in its hot end [25]. The current investigation is prompted to investigate the effects of multi-mesh regenerator on the decrease of these losses. To reach this goal, the value of the last term of Equation(6) (viscous and inertial losses) must be decreased in the hot end of the regenerator. According to the parameters of this term, effect of variations is investigated here. For a perfect stacking of  $\epsilon$  square-mesh screens in which the weaving causes no inclination of the wires and screen layers are not separated,  $\epsilon$  and  $\phi$  can be calculated as follow [26]:

$$\epsilon = \frac{4X_t - \pi}{4X_t} \tag{11}$$

$$\phi = \frac{(1 - X_t)^2}{X_t^2} = (1 + \frac{4}{\pi}(\epsilon - 1))^2 \tag{12}$$

For stationary density and mass flow rate at each section of the regenerator one can write:

$$\dot{m} = \rho V \phi A \rightarrow \phi V = \frac{\dot{m}}{\rho A} = cte \tag{13}$$

Instituting Equation (12) into the Equation (13) yields:

$$V = \frac{\dot{m}}{\rho A} (1 + \frac{4}{\pi}(\epsilon - 1))^{-2} \tag{14}$$

$$\frac{\partial V}{\partial \epsilon} = \frac{\dot{m}}{\rho A} (\frac{-8}{\pi} (1 + \frac{4}{\pi}(\epsilon - 1))^{-3}) \tag{15}$$

$$\epsilon = 0.6 \rightarrow \frac{\delta V}{\delta \epsilon} = -21.55 \frac{\dot{m}}{\rho A} \tag{16}$$

Therefore, increasing of  $\epsilon$  causes an intense decrease in  $V$ , causing  $\epsilon V$  to decrease too. Moreover, the term  $\partial p / \partial x$  is always negative, and its variations versus  $\epsilon$  can be evaluated as follow:

$$|\frac{\delta p}{\delta x}| = \frac{\mu}{\beta} |V| + \frac{1}{2} \rho C |V \cdot V| \tag{17}$$

$$\beta = \frac{2l}{33.6n\epsilon} \phi = \frac{2l}{33.6n} \frac{(1 - \frac{4}{\pi}(1 - \epsilon))^2}{\epsilon} \tag{18}$$

$$C = 0.377n(\frac{\epsilon}{\phi})^2 = 0.377n(\frac{1 - \frac{4}{\pi}(1 - \epsilon)^2}{\epsilon})^2 \tag{19}$$

According to the Equations (17) to (19), if the hot end porosity is properly increased so that Darcy Permeability ( $\beta$ ) is increased and Inertial Resistance Factor ( $C$ ) is decreased, the amount of viscous and inertial losses will be decreased. Two different modes of multi mesh regenerators whose characteristics are listed in Tables 4 and 5 have been considered in the present work.

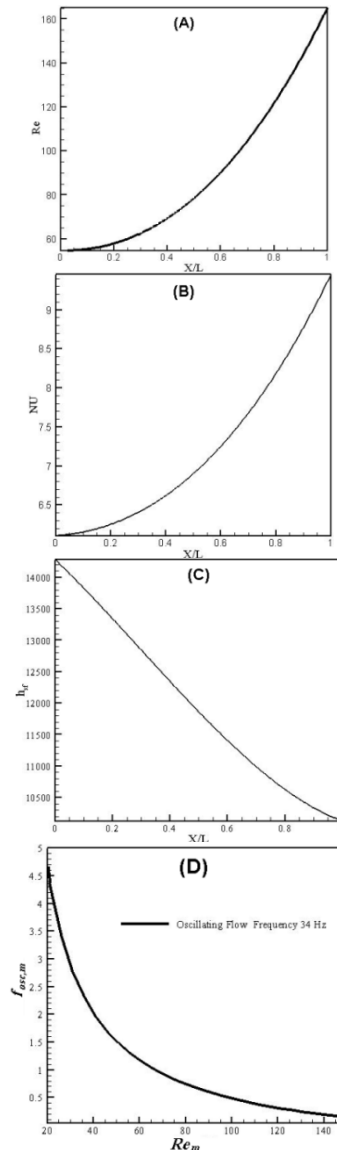


**Figure 6.** Cyclic average of A- Reynolds number, B- Nusselt number, C- convective heat transfer coefficient, and friction factor versus  $Re_m$  along the regenerator

As shown in Tables 4 and 5, porosity is decreased along the regenerator from the hot towards the cold end. This distribution is to balance the light area density of the hot end by higher area density in the cold end to reach an optimum operation of the regenerator [27]. Simulations were done under the fixed CHX wall temperature of 150 (K) for multi-mesh regenerators.

Figures 8- A, B and C show the pressure profile in the inlet and outlet of the regenerator during a cycle for uniform mesh and multi-mesh “A” and “B” regenerators, respectively. As shown in Figures 8- A to C the pressure drop of multi-mesh regenerator “A” and uniform mesh regenerator are semi-equal but the multi-mesh regenerator “B” has less pressure drop along the regenerator. Table 6 shows pressure drop and phase lag values for different regenerators.

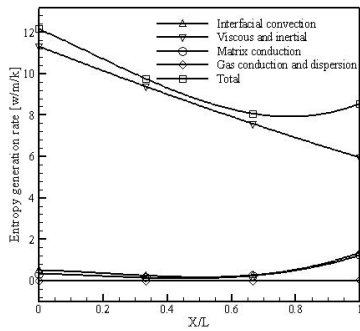


Figure 7. Cyclic average different sources of entropy generation along the regenerator

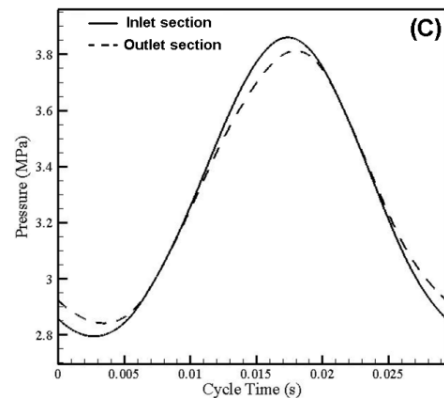
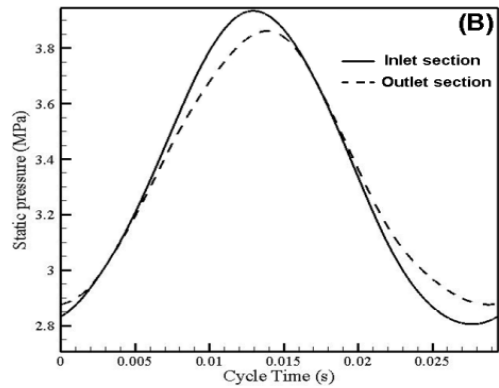
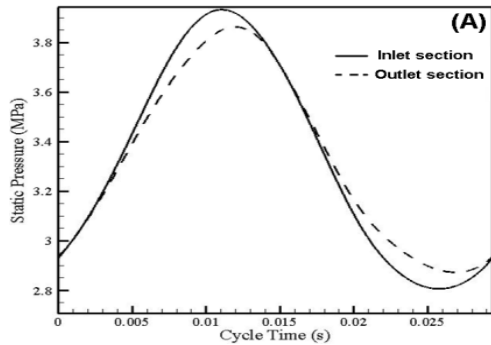


Figure 8. Pressure oscillation in the inlet and outlet sections of A- uniform mesh regenerator, B- multi-mesh “A” regenerator and C- multi-mesh “B” regenerator

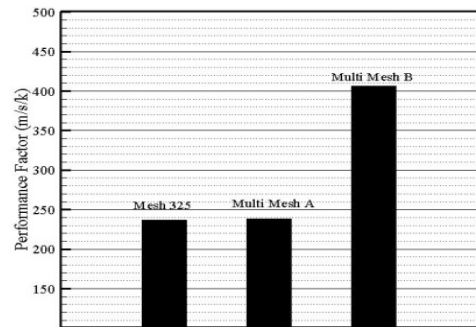


Figure 9. Performance factor of different regenerators

TABLE 4. Multi-mesh “A” properties

| Properties                      | {hot head}0 ≤ x < L/3   | L/3 ≤ x < 2*L/3        | 2*L/3 ≤ x < L           |
|---------------------------------|-------------------------|------------------------|-------------------------|
| Mesh type                       | SS spherical 60 micron  | SS Mesh 325            | SS Mesh 400             |
| ε                               | 0.7173                  | 0.6961                 | 0.692                   |
| β (m <sup>2</sup> )             | 1.543×10 <sup>-10</sup> | 1.06×10 <sup>-10</sup> | 1.005×10 <sup>-10</sup> |
| C                               | 68506.2                 | 76090                  | 103002.8                |
| Area density (m <sup>-1</sup> ) | 28300                   | 44444.44               | 48503.94                |
| D <sub>h</sub> (m)              | 152×10 <sup>-6</sup>    | 63.9×10 <sup>-6</sup>  | 57.1×10 <sup>-6</sup>   |

**TABLE 5.** Multi-mesh “B” properties

| Properties                      | {hot head} $0 \leq x \leq L/3$ | $L/3 \leq x < 2L/3$    | $2L/3 \leq x < L$       |
|---------------------------------|--------------------------------|------------------------|-------------------------|
| Mesh type                       | UMN                            | SS Mesh 325            | SS Mesh 400             |
| $\epsilon$                      | 0.9                            | 0.6961                 | 0.692                   |
| $\beta$ (m <sup>2</sup> )       | $1.86 \times 10^{-7}$          | $1.06 \times 10^{-10}$ | $1.005 \times 10^{-10}$ |
| C                               | 241.14                         | 76090                  | 103002.8                |
| Area density (m <sup>-1</sup> ) | 493.83                         | 44444.44               | 48503.94                |
| $D_h$ (m)                       | $7290 \times 10^{-6}$          | $63.9 \times 10^{-6}$  | $57.1 \times 10^{-6}$   |

**TABLE 6.** Pressure drop and phase lag values along different regenerators

| Multi-mesh “B”       | Multi-mesh “A” | Uniform mesh | Components |
|----------------------|----------------|--------------|------------|
| $X_{\Delta p}$ (KPa) | 50             | 76.5         | 80         |
| $\Delta\Phi$         | 6.12 °         | 12.24 °      | 12.24 °    |

In order to study multi-mesh regenerator behavior, cyclic average pressure drop and fluid temperature along the multi-mesh regenerator “B” is illustrated in Figures 11 and 12, respectively. As shown in Figure 11, the pressure drop is omitted in the first third span of the regenerator due to the use of media with higher porosity in this area. Besides, Figure 12 shows that there is a slight fluid temperature decrease in the hot end due to little inter-phase heat transfer area. It seems that in this area the fluid heat is lost as conduction and advection instead of storing in the solid matrix.

To investigate the operation performance of regenerators, performance factor,  $R_{osc}$  (ratio of inter-phase heat transfer to pressure drop), which is read from the Equation (20), is calculated.

$$R_{osc} = \frac{a_{sf} h_{sf}}{L_r} \tag{20}$$

Figures 9 show  $R_{osc}$  of different regenerators. According to Figures 9, the  $R_{osc}$  value of multi-mesh regenerator “B” is almost 1.7 times higher than the value of mesh 325 and multi-mesh “A”. Besides, as shown in Figures 10, the COP value of multi-mesh “B” regenerator PTC is almost 1.07 times higher than that of the others.

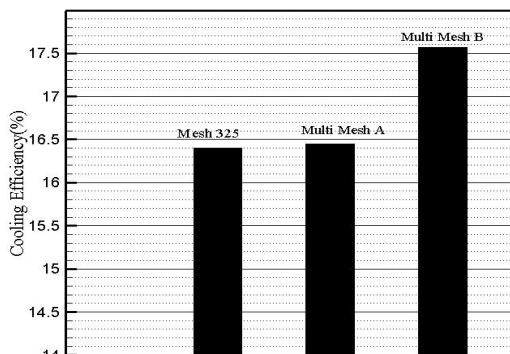


**Figure 10.** Different PTCs cooling efficiency

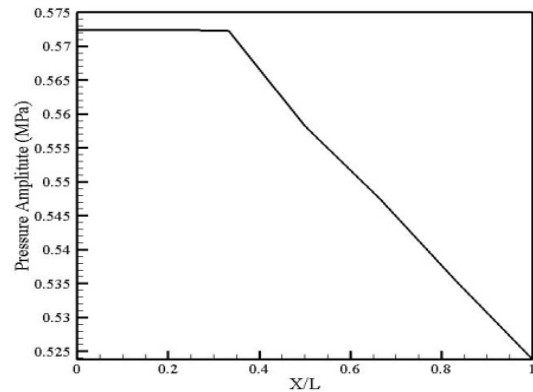


**Figure 11.** Cyclic average pressure along the multi-mesh regenerator “B”

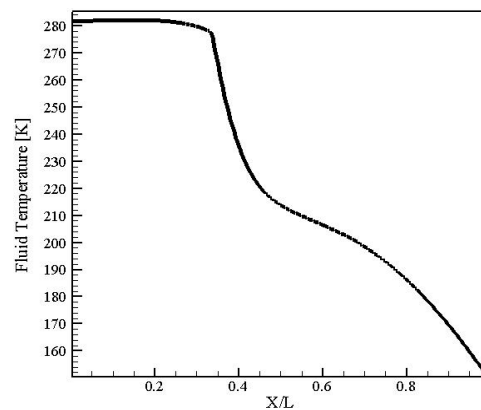


**Figure 12.** Fluid temperature variation along the multi-mesh regenerator “B”

**4. CONCLUDING REMARKS**

A single stage Stirling type ITPTC was investigated using Fluent software. In order to study the regenerator behavior and its effects on the performance of the PTC, both DEE and LTE models of heat transfer in porous medium were used. Comparison of results of DEE and

LTE models showed that DEE model is better than LTE one because it can show the sources of energy losses correctly.

For increasing performance of the regenerator, multi-mesh regenerator was studied. The porosity of medium in the hot end of the regenerator was increased to reduce the viscous and inertial losses in this area. On the other hand the porosity of its cold end was decreased to reach the proper heat transfer area between fluid and solid matrix. Two cases of multi-meshes named multi-mesh "A" and "B" were chosen. Results of simulations for fixed CHX wall temperature of 150 (K) show that  $R_{osc}$  of multi-mesh "B" and "A" and single mesh regenerators are 406, 239 and 238 (m/s.K), respectively. Corresponding COP of PTCs with multi-mesh "B" and "A" and uniform mesh regenerators are 0.1755, 0.164 and 0.164, respectively.

It is concluded that:

- Using DEE model of heat transfer in the regenerator part of the PTC is very useful because of its numeric power in revealing the amount of different energy loss sources.
- Proper use of multi-mesh regenerator improves  $R_{osc}$  of the regenerator, causing COP of the PTC to increase as well.

## 5. REFERENCES

1. Wang, C., Wu, P.Y. and Chen, Z.Q., "Numerical analysis of double inlet pulse tube refrigerator", *Cryogenics*, Vol. 33, (1993), 526–530.
2. Harvey, J.P., "Parametric Study of Cryocooler Regenerator Performance", MSc. thesis, Georgia Institute of Technology, Atlanta, Ga., (1999).
3. Siegel, R., "Influence of oscillation-induced diffusion on heat transfer in a uniformly heated channel", *Journal of Heat Transfer TRANS ASME*, Vol. 109, (1987), 244–247.
4. Khodadai, J.M., "Oscillatory fluid flow through a porous medium channel bounded by two impermeable parallel plates", *Journal of Fluids Engineering*, Vol. 113, (1991), 509–511.
5. Tanaka, M., Yamashita, I. and Chisaka, F., *JSME International Journal of Series II*, Vol. 33, (1990), 283–289.
6. Rawlins, W., "The Measurement and modeling of regenerator performance in an orifice pulse tube refrigerator", PhD. thesis, University of Colorado, Boulder, (1992).
7. Radebaugh, R., Gary, J., Marquardt, E., Louie, B., Daney, D., Arp, V. and Linenberger, D., "Measurement and calculation of regenerator ineffectiveness for temperatures of 5 to 40 K", Wright Laboratory, WPAAFB, OH, USA WL-TR-92-3074, (1992).
8. Gedeon, D. and Wood, J., "Oscillatory-flow regenerator test rig: hardware and theory with derived correlations for screens and felts", *NASA Contractor Report 198442*, (1997).
9. Zhao, T.S. and Cheng, P., *Cryogenics*, Vol. 36, (1998), 1619–1626.
10. Ju, Y.L., Wang, C. and Zhou, Y., "Numerical simulation and experimental verification of the oscillating flow in pulse tube refrigerator", *Cryogenics*, Vol. 38, (1982), 169–176.
11. Gedeon, D., "Sage pulse tube model-class reference guide", Gedeon Associates, (1999).
12. Jeong, S., Nam, K. and Jung, J., "Regenerator characterization under oscillating flow and pulsating pressure", *Cryocoolers*, Vol. 12, (2002), 531–537.
13. Nam, K. and Jeong, S., "Experimental study on the regenerator under actual operating conditions", *Advances in Cryogenic Engineering*, Vol. 47, (2002), 977–984.
14. Organ, A.J., "Thermodynamics and gas dynamics of the stirling cycle machine", *Cambridge University Press*, (1992).
15. Jeesung, C.J., "CFD simulation of multi-dimensional effects in inertance tube pulse tube cryocoolers", MSc thesis, Georgia Institute of Technology, Atlanta, Ga., (2004).
16. Etaati, M.A., "Numerical simulation of a three-stage stirling-type pulse-tube refrigerator", PhD thesis, Eindhoven University of Technology, (2011).
17. Brereton, G. and Mankbadi, R., "Review of recent advances in the study of unsteady turbulent internal flows", *Appl. Mech. Rev.*, Vol. 48, (1995), 189–212.
18. Gifford, W.E. and Longsworth, R.C., "Surface heat pumping", *Advances in Cryogenic Engineering*, Vol. 11, Plenum Press, New York, 171, (1968).
19. Fluent INC. 2003. Fluent 6 User Manual.
20. Organ, A.J., "The regenerator and stirling engine", *Cambridge University Press*, (1997).
21. Ibrahim, M. and Roy, T., "An initial non-equilibrium porous-media model for CFD simulation of Stirling regenerators", *AIAA*, (2006).
22. Yuan, K., Wang, L., Hou, Y.K. and et al., "Oscillating flow characteristics of a regenerator under low temperature conditions", *Cryocoolers 12*, edited by R. G. Ross, Jr., Plenum Academic/Plenum Publishers, New York, (2003), 539–545.
23. Taghilou, M., Ghadimi, B. and Seyyedvalilu, M.H., "Optimization of double pipe fin-pin heat exchanger using entropy generation minimization", *International Journal of Engineering Transactions C: Aspects*, Vol. 27, No 9 (2014), 1431-1438.
24. Shamsi Kooshki, M., Gandjalikhan Nassab, S.A., Ansari, A.B. "Investigation of entropy generation in a 3D laminar forced convection flow over a backward facing step with bleeding", *IJE Transactions A: Basics*, Vol. 25, No 4 (2012), 379-388.
25. Jafarian, A., Saidi M.H., Kazemzadeh Hannani, S. "Second law based analysis of fluid flow in the regenerator of pulse tube refrigerator", *International Journal of Engineering Transactions A: Basics*, Vol. 21, No 2 (2008), 181-194.
26. Robbert, A.A., "Cryogenic regenerative heat exchangers", *New York: Plenum Press*, (1997), 48–54.
27. Tao, Y.B. and Liu, Y.W., "Numerical analysis on pressure drop and heat transfer performance of mesh regenerators used in cryocoolers", *Cryogenics*, Vol. 49, (2009), 497–503.



## CFD Simulation of a Multi-mesh Pulse Tube Regenerator

RESEARCH  
NOTEB. Mousavi<sup>a</sup>, A. A. Alemrajabi<sup>b</sup>, A. Jafarian<sup>c</sup>, M. Arablu<sup>d</sup>, A. Behjatian<sup>e</sup><sup>a</sup>Department of Civil Engineering, University of Colorado Denver, Denver<sup>b</sup>Department of Mechanical Engineering, Isfahan University of Technology, Isfahan<sup>c</sup>Department of Mechanical Engineering, Tarbiat Modares University, Tehran<sup>d</sup>Department of Mechanical Engineering, University of North Carolina Charlotte, Charlotte<sup>e</sup>Department of Mechanical Engineering, Southern Illinois University, Carbondale

## P A P E R I N F O

## چکیده

*Paper history:*

Received 07 May 2013

Accepted in revised form 18 September 2014

*Keywords:*

Pulse Tube

Cryocooler

Multi Mesh Regenerator

Oscillating Flow

طی دو دهه اخیر، سردساز لوله ضربانی لوله اینرتنسی به دلیل قابلیت اعتماد بالا کاربرد بسیار وسیعی در صنایع هوا فضا یافته است. به همین جهت تلاش‌های زیادی در جهت توسعه این سیستم صورت گرفته است. بررسی‌ها نشان داده است که بیشترین تلفات این سیستم در قسمت بازیاب که محیطی متخلخل است صورت می‌گیرد. به دلیل پیچیدگی فیزیک این تلفات، اثرات بازده بازیاب بر عملکرد سردساز با استفاده از روش CFD مورد بررسی قرار گرفت. جهت محاسبه انتقال حرارت جایجایی در محیط بازیاب از هر دو روش تک معادله‌ای و دو معادله‌ای بهره گرفته شد. محاسبه نرخ تولید انترپی در محیط متخلخل بازیاب نشان داد که ۸۵٪ تلفات بازیاب ناشی از تلفات ویسکوز و اینرسیال است و همچنین مقدار این تلفات در انتهای گرم بازیاب اتفاق می‌افتد. بنابراین، به منظور بهبود عملکرد سردساز روش بازیاب با مش چندگانه مورد مطالعه قرار گرفت. نتایج حاصل از شبیه‌سازی‌ها تحت شرایط دمایی ۱۵۰ کلوین دیواره CHX مقدار ضریب عملکرد سردساز با بازیاب با مش چندگانه بهینه ۱/۰۷ برابر سردساز ساده است. مقایسه نتایج شبیه‌سازی‌ها با مقادیر آزمایشگاهی و مقادیر عددی منتشر شده در نشریات درستی نتایج شبیه‌سازی حاضر را تایید کرد.

**doi:** 10.5829/idosi.ije.2014.28.01a.16